SPE 68076

The Application of Buckley-Leverett Displacement to Waterflooding in Non-Communicating Stratified Reservoirs

Noaman A.F. El-Khatib, SPE, King Saud U.

This paper was prepared for presentation at the 2001 SPE Middle East Oil Show held in Bahrain, 17–20 March 2001.

Abstract

A mathemathematical model is developed for performance prediction of waterflooding performance in stratified reservoirs using the Buckley-Leverett displacement mechanism. A modified definition of the mobility ratio is untroduced to account for the saturation variation behind the displacement front. Using this modified mobility ratio, the Dykstra-Parsons equations can be used to estimate the relative locations of the displacement fronts in different layers at the time of water breakthrough at a given layer. For layers after water breakthrough, expressions for the flow rate and water throughput are derived in terms of integral equations that are solved by iteration. The Buckley-Leverett and Welge tangent method is used to obtain the outlet and average saturations in each layer. These saturations are used to obtain the fractional oil recovery and water cut of each layer. Summation over all layers yields the performance of the total system. Expressions for the injectivity ratio are also derived.

Solutions for stratified systems with log normal permeability distribution were obtained and compared with those for the piston-like displacement (Dykstra-Parsons). The effects of viscosity ratio and the Dykstra-Parsons permeability variation coefficient (V_{DP}) on the performance is investigated. The Introduction of pseudo relative permeability functions is discussed.

Introduction

Petrophysical properties of oil-bearing formations are normally heterogeneous. The most significant property that affects waterflooding performance is the absolute permeability and its variation normal to the direction of flow. This variation causes the displacing fluid to advance faster in zones of highr permeability and thus results in earlier breakthrough in such layers. In this case, the conventional frontal advance theory of Buckley-Leverett[1] and its graphical equivalent of Welge tangent construction method[2] cannot be applied to the reservoir as a single layer. The reservoir is divided into a number of layers, each is assumed to be homogeneous with a constant permeability.

Different analytical models are available in the literature for waterflooding performance of stratified reservoirs[3-10]. Stiles[3]assumed the displacement velocity in a layer to be proportional to its absolute permeability neglecting the effect of mobility ratio.Dykstra and Parsons[4] developed a model for noncommunicating layers without crossflow between layers while Hiatt[5] presented a model for communicating layers with complete crossflow. Warren and Cosgrove[6] applied Hiatt's model to stratified systems with a log normal permeability distribution. Hearn[7] developed expressions for the pseudo relative permeabilty functions for communicating stratified reservoirs. Reznik et al.[8] extended the Dykstra-Parsons method to continuous real-time basis. El-Khatib[9,10] investigated the effect of crossflow on the performance of stratified reservoirs and presented a closed form analytical solution for communicating stratified systems with log-normal permeability distributions.

All of the above mentioned models used to predict waterflooding performance in stratified reservoirs assume piston-like displacement in the different layers of the reservoir. Under this assumption, only oil flows ahead of the displacement front with a relative permeability k^0_{ro} at the irreducible water saturation. All recoverable oil is displaced by water leaving only the reidual oil saturation behind the displacement front with water flowing with a relative permeability k^0_{rw} at the residual oil saturation. Only the end points of the rock relative permeability data k^0_{ro} and k^0_{rw} are used in these models. These two values with oil and water viscosities define the mobility ratio which is an important factor affecting the performance. When the displacement front in a given layer reaches the outlet face (producing well), no more oil flows from that layer and the production is completely water. All the recoverable oil ($1 - S_{wi} - S_{or}$) is produced from the layer at the time of water breakthrough. This leads to a highly optimistic performance predictio, i.e.

higher fractional recovery and lower water cut. This is particularly aggrevated at high (unfavorable) mobility ratios where early breakthrough occurs with appreciable amounts of recoverable oil left behind the displacement front.

As opposed to piston-like displacement, the frontal advance theory shows that the saturation at the displacement front S_w^* is less than $(1 - S_{or})$ and is determined by drawing a tangent to the fractional flow curve ($f_w - S_w$) from the point of initial conditions (S_{wi}, 0). The point of tangency determines the outlet water saturation and water cut, S_w^* and f^*_w at the time of water breakthrough. The intercept of the tangent with the horizontal line of f_w=1 determines the average saturation S_w which is also below $(1 - S_{or})$. The oil recovery from the layer at time of breakthrough is $(S_w - S_{wi})$ and is equal to the recoprical of the slope of the tangent line. After breakthrough, as water injection continues, more of the oil that is left behind the displacement front is recovered and the water fraction f_w increases steadily approaching the value of one as the oil recovery approaches the ultimate oil recovery of $(1 - S_{wi} - S_{or})$. The outlet saturation S_{wl} and the water cut f_{wl} at any time after breakthrough are those at the point of tangency to the fractional flow curve of a line with slope equals to the recoprical of the pore volumes of water injected into the layer (dimensionless time). Again, the intercept of the tangent with the horizontal line of f_w=1 locates the average saturation which determines the oil recovery at that time.

The difficulty of applying the frontal advance method to a stratified system with several layers stems from the fact that at a given time, each layer would be at a different stage of displacement conditions. It is required to estimate the pore volumes of water injected into the different layers at a given real time. Since no crossflow is allowed between different layers in noncommunicating systems, each layer can be treated individually. The waterflooding performance in terms of fractional recovery and water cut vs. dimensionless time relative to each layer is the same for all layers. The problem is to find the dimensionless time in each layer at a given real time and to add recovered oil volumes and water flow rates to obtain the overall performance of the reservoir. Such a procedure was presented by Willhite[11] and uses tables for the performance of the different layers to lookup and interpret performance. This method is clearly inadqute for automatic computations. Snyder and Ramey[12] used a one-dimensional finite difference numerical simulator to solve for the water saturation in each layer and combined the cells in a series-parallel pattern.

In this work an exact analytical solution is presented for the flow rates in the different layers before and after water breakthrough. Expressions are also derived for the relative dimensionless times and front locations in the different layers at a given instant of real time (i.e. time of brakthrough in a given layer). Once the dimensionless time in a layer is estimated, the frontal advance procedure is used to determine oil recovery and water cut from that layer. Since this is done for all layers at the same time, a simple summation over all layers results in the performance of the stratified system. To perform the computations in analytical rather than graphical manner, all needed is to express the relative permeability curves in forms of algebraic equations.

Assumptions

The following assumptions are made:

1. The system is linear, horizontal and of constant thickness.
2. The flow is isothermal, incompressible and obeys Darcy's law.
3. Capillary and gravity forces are negligible
4. The system is devided into a number of homogeneous layers each with uniform thickness and constant permeability.
5. The system is a noncommunicating with no crossflow allowed between the different layers.
6. The relative permeability characteristics are the same for all layers.
7. The initial fluid saturation is uniform at the irreducible water saturation.
8. The porosity is assumed constant in all layers.

For convenience, the layers are arranged in decreasing order of permeability. The examples presented in this paper are for log- normal permeability distributions. However, the procedure developed can be applied for any arbitrary distribution.

Mathematical Model

The basic equations of the mathematical model are presented in this section. A detailed derivation of the model is given in the appendix.

Performance before Water Breakthrough. Before water breakthrough in the first(most permeable) layer, the location of the displacement front in any layer j ,X_{fj} in terms of X_{f1} is given by

$$X_{fi} = \left(\frac{\bar{\gamma}}{\bar{\gamma}-1}\right)\left[1-\sqrt{1-2\left(\frac{\bar{\gamma}-1}{\bar{\gamma}}\right)\frac{k_i}{k_1}\left(X_1-\left(\frac{\bar{\gamma}-1}{2\bar{\gamma}}\right)X_1^2\right)}\right] \quad (1)$$

The dimensionless time of the different layers is given by

$$t_{Di} = X_{fi} t_D^* \quad (2)$$

The fractional oil recovery R and total dimensionless time τ are given by

$$\tau = \frac{\sum_{i=1}^{n} t_{Di}\Delta h_i}{h_t} \quad (3)$$

and

$$R = \tau \quad (4)$$

The expression for the injectivity ratio I_R is

$$I_R = \frac{1}{c_t}\sum_{i=1}^{n}\frac{k_i\Delta h_i}{1-\left(\frac{\bar{\gamma}-1}{\bar{\gamma}}\right)X_i} \quad (5)$$

During this period

$$f_w = 0 \tag{6}$$

Performance after Water Breakthrough. At the time of breakthrough in layer j, the location of the displacement front for lyer i (j<i≤n) is given by

$$X_{fi} = (\frac{\bar{\gamma}}{\bar{\gamma}-1})[1-\sqrt{1-(\frac{\bar{\gamma}^2-1}{\bar{\gamma}^2})\frac{k_i}{k_j}}] \tag{7}$$

The dimensionless times t_{Di} for these layers are obtained by applying Eq.(2) to each layer.

For the layers i=1,2,…….,j-1,

$$\Delta\eta_i = \frac{k_i}{k_{j-1}}\Delta\eta_{j-1} \tag{8}$$

$$\Delta\eta_{j-1} = \eta_{j-1} = \frac{t_D^*}{\lambda_o^0}(\frac{\bar{\gamma}+1}{2\bar{\gamma}})[\frac{k_{j-i}}{k_j}-1] \tag{9}$$

and

$$\eta_i = \eta_{i\,old} + \Delta\eta_i \tag{10}$$

where η is a function of the dimensionless time t_{Di} as defined by the integral equation, Eq.(A-30). The dimensionless times t_{Di} for these layers are obtained by solving Eq.(A-30) numerically for each layer. Using the definition of the integral I ,Eq.(A-9), and integration by parts, Eq.(A-30) can be expressed in a form more convenient for iterative solution.

$$\eta_i = 0.5\left(t_{Di}^2 I(1/t_{Di}) - t_D^{*2} I^* - \int_{1/t_D^*}^{1/t_{Di}} \frac{df_w'}{\lambda_t f_w'^2}\right) \tag{11}$$

Equation (11) is solved for t_{Di} by the Newton-Raphson method where the integral is evaluated numerically to obtain the value of η for an assumed value t_{Di} . A corrected value of t_{Di} is obtained using the iteration scheme

$$f(t_{Di}) = \eta_i - 0.5\left(t_{Di}^2 I(1/t_{Di}) - t_D^{*2} I^* - \int_{1/t_D^*}^{1/t_{Di}} \frac{df_w'}{\lambda_t f_w'^2}\right) = 0 \tag{12}$$

$$t_{Di}^{\ new} = t_{Di}^{\ old} - \frac{f(t_{Di})}{f'(t_{Di})} \tag{13}$$

From Eq.(A-30)

$$f'(t_{Di}) = -t_{Di} I(1/t_{Di}) \tag{14}$$

The dimensionless time for the total system τ is obtained from the individual layers dimensionless times using Eq.(3). The frontal advance theory is applied to layers 1≤i≤ j to obtain the outlet saturation and water cut by drawing a tangent to the fractional flow curve with slope $1/t_{Di}$. The average saturation in each of these layers is also obtained from the intersection of the tangent at f_w=1. The computations are carried out numerically using analytical equations for the relative permeability curves.

Using Eqs. (A-13) and (A-27) for the total flow rates in layers before anf after breakthrough respectively, the water cut for the system is given by

$$f_{wj} = \frac{\sum_{i-1}^{j}\frac{k_i\Delta h_i}{t_{Di}I(1/t_{Di})}f_{wi}}{\sum_{i-1}^{j}\frac{k_i\Delta h_i}{t_{Di}I(1/t_{Di})} + \lambda_o^0\sum_{i-1}^{j}\frac{k_i\Delta h_i}{\sqrt{1-(\frac{\bar{\gamma}^2-1}{\bar{\gamma}^2})\frac{k_i}{k_j}}}} \tag{15}$$

The fractional oil recovery (in PV) can be expressed as

$$R_j = \frac{1}{h_t}\left\{\sum_{i=1}^{j}(\bar{S}_w - S_{wi})\Delta h_i + t_D^*\sum_{j+1}^{n}X_{fi}\Delta h_i\right\} \tag{16}$$

The injectivity ratio can be expressed as

$$I_R = \frac{\sum_{i-1}^{j}\frac{k_i\Delta h_i}{t_{Di}I(1/t_{Di})} + \lambda_o^0\sum_{i-1}^{j}\frac{k_i\Delta h_i}{\sqrt{1-(\frac{\bar{\gamma}^2-1}{\bar{\gamma}^2})\frac{k_i}{k_j}}}}{\lambda_o^0 c_t} \tag{17}$$

Conversion to Real Time.

For Constant Injection Rate:

$$t = \frac{A_t L\varphi\tau}{q_t} \tag{18}$$

$$\Delta P_t = (\Delta P_t)_{in}/I_R \tag{19}$$

For Constant Pressure Drop

Before breakthrough in the first layer

$$t = \frac{L^2\varphi\, t_D^*}{k_1\lambda_o^0\Delta P_t}[X_1 - (\frac{\bar{\gamma}-1}{2\bar{\gamma}})X_1^2] \tag{20}$$

At time of breakthrough in layer j

$$t_j = (\frac{\bar{\gamma}+1}{2\bar{\gamma}})\frac{L^2\varphi\, t_D^*}{k_j\lambda_o^0\Delta P_t} \tag{21}$$

$$q_t = (q_t)_{in} I_R \tag{22}$$

Results and Discussion

The relative permeability relations used in this study are

$$K_{rw} = 0.5\ S_D^3 \tag{23}$$

$$K_{ro} = (1-S_D)^2 \tag{24}$$

where

$$S_D = \frac{S_w - S_{wi}}{1-S_{wi}-S_{or}} \tag{25}$$

Figure 1 shows the relative permeability, the fractional flow and the total mobility curves for an oil/water viscosity ratio of 2.5. It is to be noted that the mobility ratio as defined for piston-like displacement does not apply for the case of Bucley-Leverett displacement. In this case, the oil and water mobilities in the flooded zone are not constant but vary from the values of λ^{o}_{w} and zoro at the injection point to the values of λ^{*}_{w} and λ^{*}_{o} at the oil/water interface. The oil mobility of the unflooded zone is constant at λ^{o}_{o} with $\lambda_{w} = 0$. The effective mobility ratio for the displacement $\bar{\gamma}$ as defined by Eq.(7) is based on an average total mobility in the invaded zone as given by Eq.(6). Table 1 shows the values for the mobilities at different zones in the reservoir as well as the conventional and effective mobility ratios for different values of oil viscosities with a water viscosity of 1 cp.

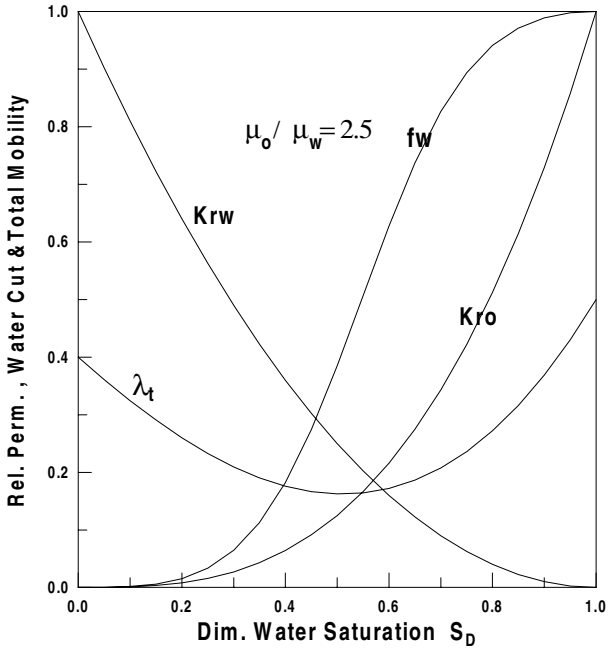

Fig. 1 - Rel. Perm., Water Cut ant Total Mobility Curves

Figures 2-4 show the performance results for a run with oil/water viscosity ratio of 2.5 and permeability variation coefficient V_{DP} of 0.5 for both piston-like and Buckley-Leverett displacement. This corresponds to a mobility ratio of 1.25 for piston-like and 0.75 for Buckley-Leverett displacement.

Figure 2 shows the fractional oil recovery (vertical coverage) as function of the dimensionless time τ. Oil recovery is reported in terms of the recoverable oil volume ($1 - S_{wi} - S_{or}$). Before B.T. in the first layer, oil recovery for both B-L and piston like displacement is equal to the dimensionless time since all injected water remains in the reservoir and an equal amount of oil is produced. Earlier breakthrough will occur in the case of B-L displacement. This is because not all of the recoverable oil is displaced from the invaded zone in the BL case and so the injected water will move faster. As the displacement process continues, more of the oil left behimd the displacement front will be recovered and eventually all recoverable oil will be produced. This however will take longer time (PV injected) than for the PL case in which oil recovery reaches unity when water B.T. occurs in the last layer. The fractional oil recovery in the B-L displacement case does not reach a value of one at that time.

Table 1 . Mobilities and Mobility Ratios

μ_o cp.	10	5	2.5	1	0.5
λ^{0}_{w}	0.5	0.5	0.5	0.5	0.5
S_D^{*}	0.560	0.653	0.743	0.848	0.907
f_w^{*}	0.8198	0.8520	0.8863	0.9292	0.9555
λ^{*}_{t}	.107278	.163101	.231702	.327778	.390193
$\bar{\lambda}_{t}$	.159054	.277101	.300333	.386197	.432851
λ^{0}_{o}	.1	.2	.4	1.0	2.0
γ	5.0	2.5	1.25	0.5	0.25
$\bar{\gamma}$	1.5905	1.1355	0.7508	0.3862	0.2164

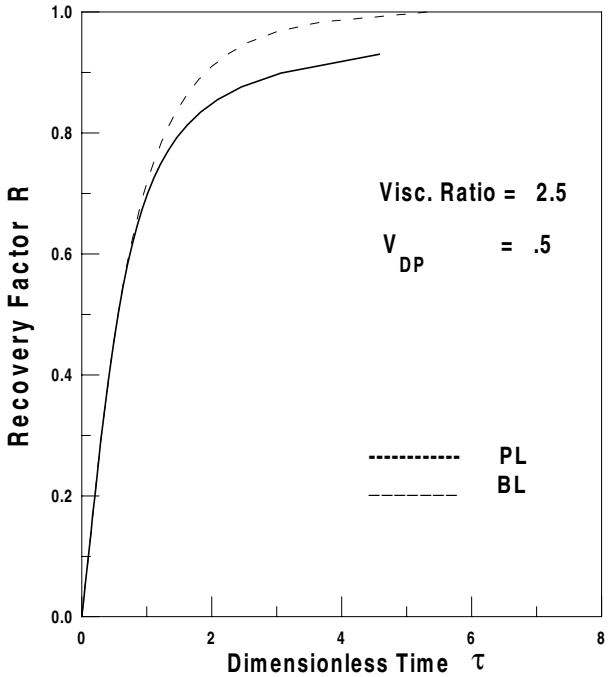

Fig.2 - Recovery Factor vs. Dimensionless Time

Figure 3 shows the water cut f_w vs. oil recovery. At early stages of displacement, the values of f_w in the case of B-L displacement is lower than that for the PL case. This is

because while it is unity for PL case. in the successive layersare are less than the corresponding values for a piston-like displacement process. This is due to the assumption of 100% water production from the flooded layers in case of piston-like displacement while the value of f_w at breakthrough for BL case is f_w^*(f_w^* <1) .As the layers will continue to produce water and oil after water breakthrough in the case of B-L displacement f_w continues to increase and surpasses the value for the PL case at later stages of displacement. When the last layer is flooded, the value of f_w reaches unity in the piston-like displacement but remains below unity in B-L displacement.

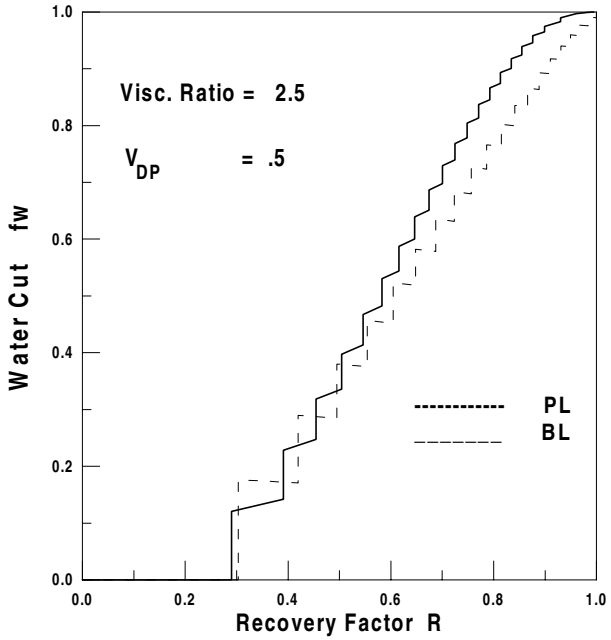

Fig.3- Water Cut vs. Recovery Factor

Figure 4 shows the injectivity ratio I_R vs. dimensionless time for PL and BL displacements. The injectivity ratio starts at a value of onefor both cases. There is a continuous increase of the injectivity ratio for the piston-like displacement case and a value of 1.25 (the mobility ratio for this run) is reached at the end of displacement as predicted theoretically.As discussed earlier, the definition of mobility ratio for the piston-like displacement does not apply for the B-L displacement case. As shown in Table 1, the total mobility at the injection point λ_w^o is 0.5 (corresponding to a water viscosity of 1). At the displacement front, the total mobility corresponding to the breakthrough saturation is 0.2317. The average total mobility in the invaded zone is .3 . The mobility in the uninvaded zone is 0.4. This will give an of 0.75 The injectivity ratio in the BL case decreses below unity because of this low effective mobility ratio (<1) . The injectivity ratio reaches a minimum value before it starts increasing again. After water breakthrough in the different layers, the water saturation continues to increase approaching its value at the injection end and the total mobility would increase as seen from Fig 1. Ultimately, for BL case will reach the value of 1.25 which corresponds to PL displacement but this requires a large PV of water injection.

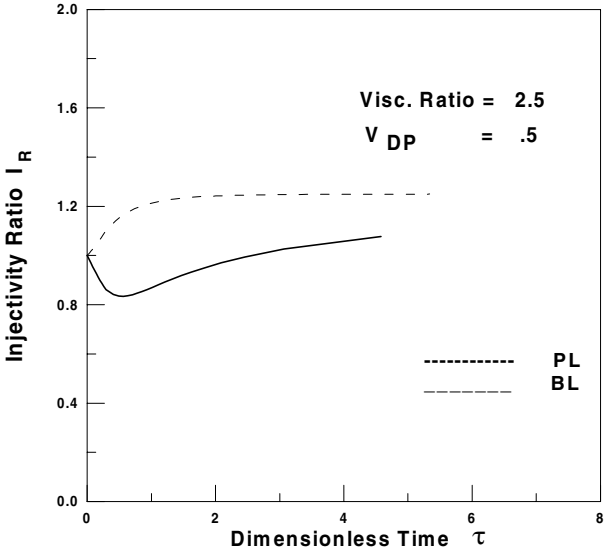

Fig.4 -Injectivity Ratio vs. Dimensionless Time

Effect of Viscosity Ratio

Figure 5 shows the fractional oil recovery vs. dimensionless time for oil/water viscosity ratios of 10,2.5 and 0.5 at a constant V_{DP} value of 0.5. As expected, oil recovery decreases as the viscosity ratio and hence mobility ratio increases. Oil recovery is lower for BL displacement than for PL displacement as was explained before. The difference beween the two cases however decreases at lower viscosity ratios (favorable mobility ratios).

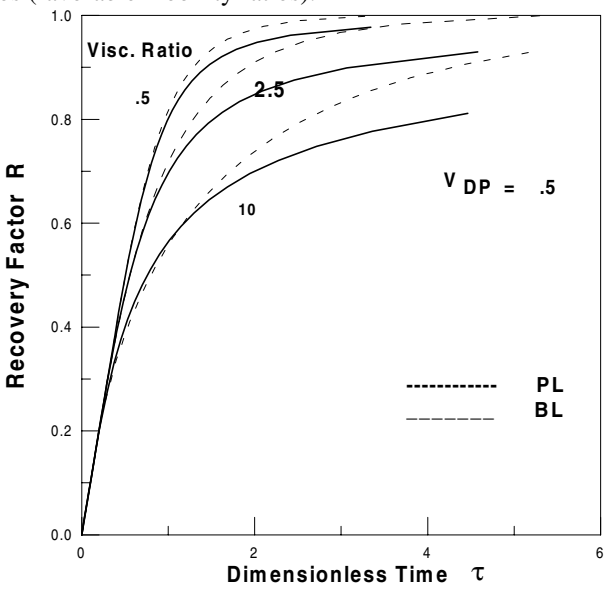

Fig.5 - Effect of Visc. Ratio on Recovery Factor

Figure 6 shows the water cut f_w vs. the recovery factor for the different values of oil / water viscosity ratios. The water

cut f_w is higher at higher mobility ratios for both BL and PL cases. At high viscosity (mobility) ratios, the difference between the two cases is appreciable due to early breakthrough and lower water saturation at the displacement front. However, at low viscosity ratios , the oil saturation at the displacement front approaches the residual oil saturation and f_w for the BL displacement is almost identical to that of PL case.

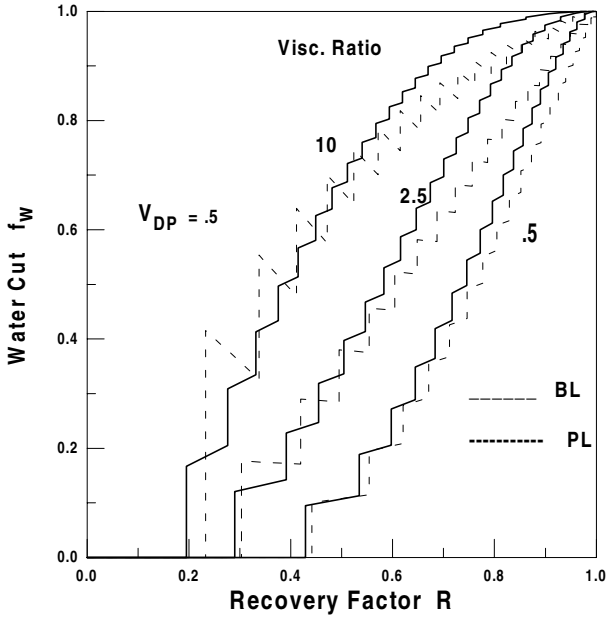

Fig. 6 - Effect of Visc. Ratio on Water Cut

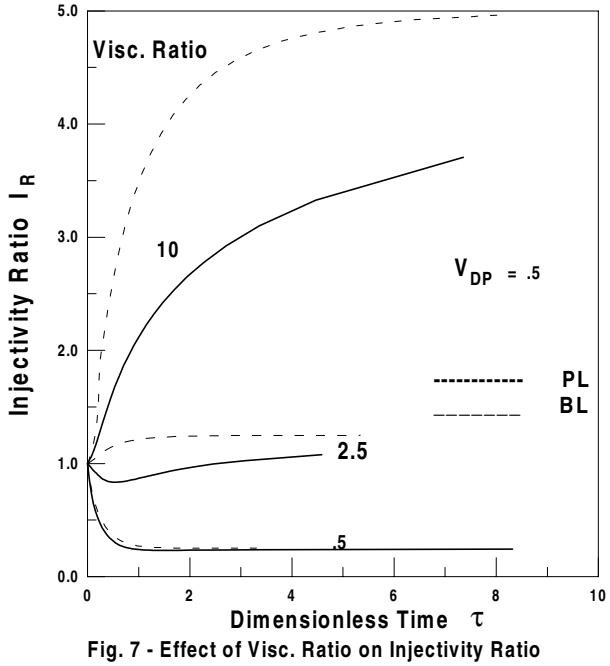

Fig. 7 - Effect of Visc. Ratio on Injectivity Ratio

Figure 7 shows the injectivity ratio I_R vs. dimensionless time for the different values of oil/water viscosity ratios. For PL displacement, the injectivity ratio increases with time for unfavorable (> 1) and decreases for favorable (< 1) mobility ratios . At the time of breakthrough in the last layer, the injectivity ratio reaches a value equal to the mobility ratio γ . For BL displacement, the injectivity ratio is always lower than that for the PL case. At early times, the modified mobility ratio $\bar{\gamma}$ is the controlling factor and the injectivity ratio will decrease with time if $\bar{\gamma}$ is less than unity. For the viscosity ratio of 2.5, although the PL mobility ratio is 1.25, the modified mobility ratio $\bar{\gamma}$ is 0.75 and so I_R starts declining with time untill it reachrs a minimum. After a number of layers are flooded and the water saturation in these layers increases above the breakthrough saturation, the total mobility increses and the injectivity starts increasing and approaches that for the PL case. It is also to be noted that the difference between the BL and PL cases diminishes at low viscosity (mobility) ratios as seen from the curve for 0.5 viscosity ratio.

Effect of Permeability Variation

Figure 8 shows the fractional oil recovery vs. dimensionless time for values of V_{DP} of 0.1, 0.5,0.9 at an oil/water viscosity ratios of 10. Oil recovery decreases as the value of V_{DP} increases i.e as the system becomes more heterogeneous. Although the fractional oil recovery ultimately reaches a value of 1, it takes much more time to approach this value for the more heterogeneous reservoirs due to the large contrast between the permeabilities of the different layers for such reservoirs..As expected, the oil recovery after breakthrough is lower for BL displacement than for PL displacement. The difference between the two cases increases at lower values of V_{DP}, i.e. for more homogeneous systems.

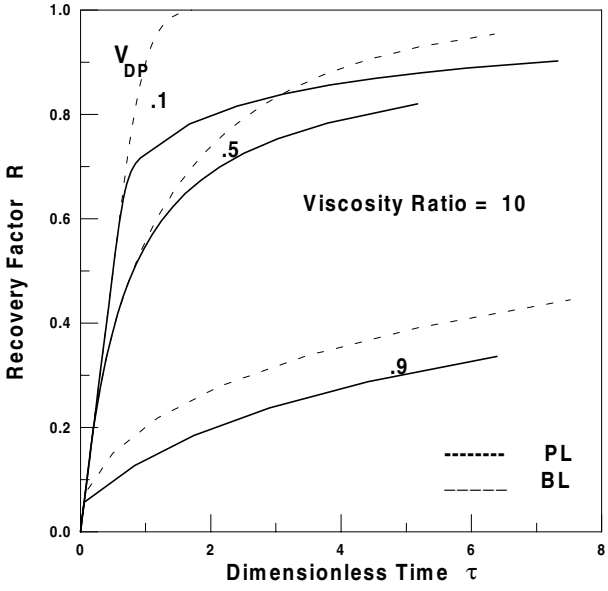

Fig. 8 - Effect of Perm. Variation on Recovery Factor

Figure 9 shows the water cut f_w vs. the recovery factor for the different values of V_{DP}. Earlier breakthrough and higher

water cuts are observed for heterogeneous reservoirs (higher values of V_{DP}). The departure of the BL and PL curves is more significant for the lower values of V_{DP}, i.e. for homogeneous reservoirs.

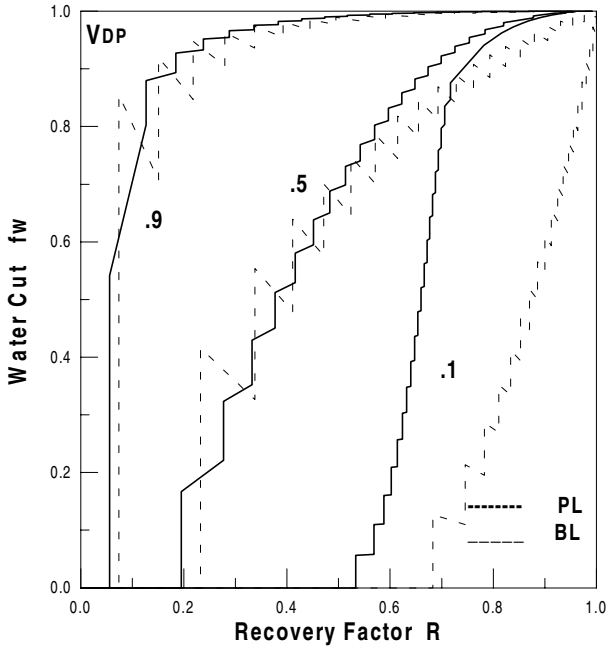

Fig. 9 - Effect of Perm. Variation on Water Cut

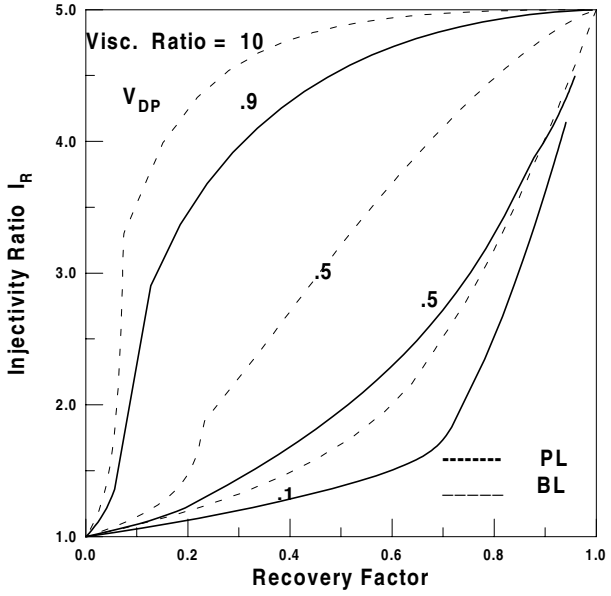

Fig. 10 - Effect of Perm. Variation on Injectivity Ratio

Figure 10 shows the injectivity ratio I_R vs. the recovery factor for the different values of V_{DP}. The injectivity ratio increases continuously from unity at the beginning to the ultimate value of γ=5 for corresponding to the viscosity ratio of 10. The injectivity ratio increases as heterogeneity (V_{DP}) increases. The injectivity ratio is always higher for the PL case than that for the BL case at the same value of R. A change in the slope of the curves is observed after water breakthrough.

Pseudo Relative Permeability and Fractional Flow Curves. The main idea behind the concept of pseudo functions is to reduce the dimensionality of computational model by averaging properties in the vertical direction. Hearn[7] introduced pseudo relative permeability curves for Figure 10 communicating stratified resevoirs. These functions reproduce the behavior of the system under piston like displacement assumptions. For more complicated systems, the pseudo fuctions should be time dependent (dynamic) as shown by many investigators. Even for Piston like displacement without crossflow, Pande et al.[13] found that the static psudo functions do not apply for mobility ratios other than unity.

Equation (15) gives the water cut at the outlet face at the time of breakthrough in layer j. The lumped (pseudo or average) water saturation at the outlet face at that time is

$$\tilde{S}_j = Sw_i + \frac{\sum_{m=1}^{j} \Delta h_m (Sw_m - Sw_i)}{h_t} \qquad (26)$$

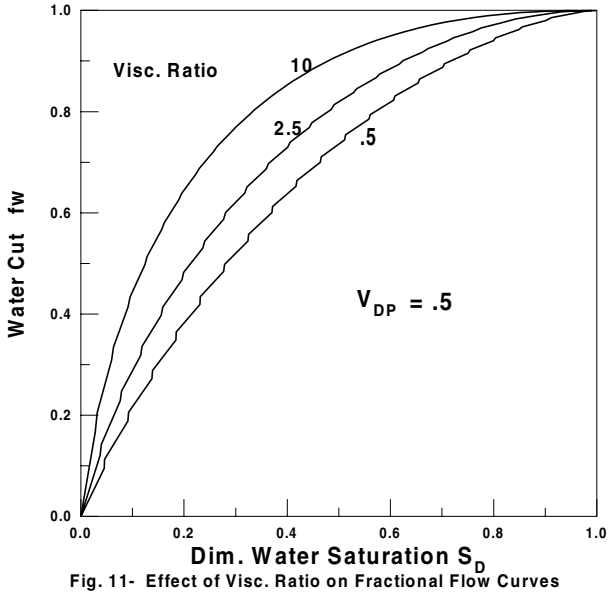

Fig. 11- Effect of Visc. Ratio on Fractional Flow Curves

Figure 11 shows the fractional flow curves constructed for BL displacement at different values of viscosity ratios. Careful investigation shows that the curves are not smooth. A sudden jump occurs at times of breakthrough and continuous increase in both saturation and f_w occurs between times of breakthrough in the successive layers. Figure 12 shows the curves at a viscosity ratio of 10 for different values of permeability variation. The figure shows higher water cuts at the same value of water saturation for the more heterogeneous reservoirs.

Average or pseudo relative permeability functions may be estimated at the outlet face saturations by requiring the same flow rates of oil and water in a homogeneous system with the same dimensions and average absolute permeabilty as the stratified system and under the same total pressure drop. From

the model equations the following expressions may be obtained.

$$\frac{\tilde{k}_{rw}}{k^0_{rw}} = \frac{I_R f_w}{\gamma} \tag{27}$$

$$\frac{\tilde{k}_{ro}}{k^0_{ro}} = I_R(1-f_w) \tag{28}$$

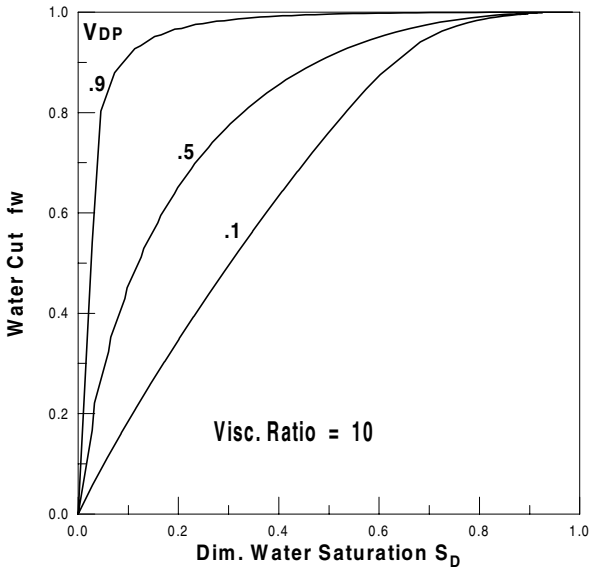

Fig. 12 - Effect of Perm. Variation on Fractional Flow Curves

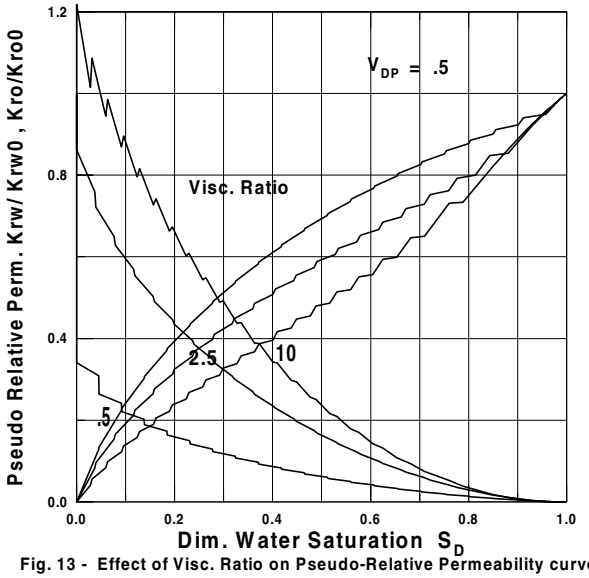

Fig. 13 - Effect of Visc. Ratio on Pseudo-Relative Permeability curves

Figure 13 shows the pseudo relative permeability curves for different values of viscosity ratios. It is observed that the viscosity ratio has a significant effect on the pseudo relative permeabilities contrary to Hearn's pseudo functions. Increasing the viscosity ratio incrases the pseudo relative permeability of the oil phase and increases that of the water phase.

Figure 14 shows the pseudo relative permeability curves at a viscosity ratio of 10 for different values of permeability variation. Incresing reservoir heterogeneity decrases the pseudo relative permeability of the oil phase and increases that of the water phase.

Figures 13 and 14 show a pseudo oil relative permeability higher than unity at zero dimensionless water saturation for high viscosity ratios (effective mobility ratio > 1). This is due to the increase of injectivity as the displacement fronts advance in the different layers while the water saturation remains at its initial value untill water breakthrough occurs at the first layer. For effective mobility ratios less than unity, the opposite occurs and the pseudo relative permeability for oil drops below unity at initial water saturation.

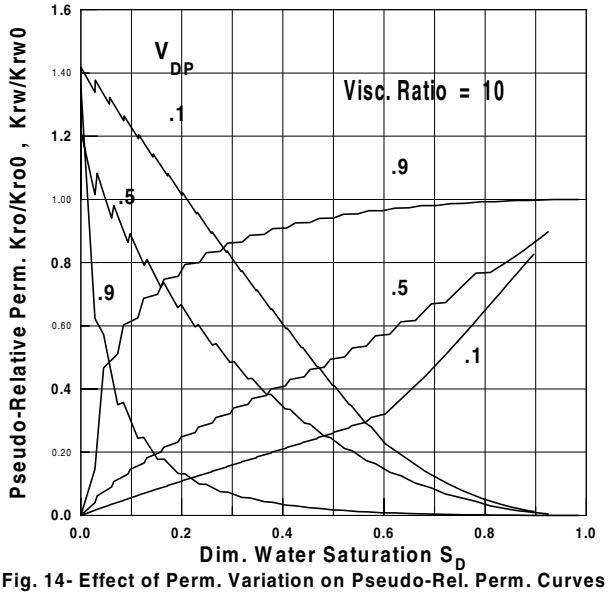

Fig. 14- Effect of Perm. Variation on Pseudo-Rel. Perm. Curves

As stated earlier, the fractional flow and pseudo oil relative permeability curves derived correspond to conditions at X=1 at different times and thus cant be applied for the entire system. To show that such functions do not reproduce the same performance if applied to a homogeneous system, we consider the average water saturatios as obtained from the frontal advance method for a layer i.

$$(\bar{S}_w)_i = (S_{wl})_i + (1-f_{wi})t_{Di} \tag{29}$$

Equation (29) is the analytical equivalence of the graphical tangent construction method of Welge. If we write Eq.(29) for each layer, multiply each equation by the corresponding layer's pore volume, add all the equations and devide by the total pore volume , the following equation is obtained

$$\bar{S}_w = S_{wl} + (\tau - \sum_{i=1}^{j} \frac{\Delta h_i}{h_t} t_{Di} f_{wi}) \tag{30}$$

In order that the same performance is reproduced we must have

$$\sum_{i=1}^{j} \frac{\Delta h_i}{h_t} t_{Di} f_{wi}) = \tau\ f_w \qquad (31)$$

It is apparent from equations (3) and (15) that equation (31) is not satisfied. We can therefore conclude that the pseudo functions derived can only be applied to predict the behavior al the outlet face (production well).

Conclusions

1. A mathematical model is developed for applying the Buckley-Leverett frontal advance theory to immiscible displacement in noncommunicating stratified reservoirs. The developed model gives more accurate results as compared to conventional models that assume piston like displacement.
2. An effective mobility ratio based on the average total mobility in the invaded zone is introduced to account for variable saturation behind the displacement front. This effective mobility ratio rather than the conventional mobility ratio controls the BL displacement before water breakthrough. Using this effective mobility ratio, Dykstra-Parsons equations can be applied to determine the locations of the displacement fronts in the different layers before breakthrough.
3. Oil recovery after breakthrough and water cut are always less for BL displacement than those for PL displacement with the difference becoming more noticeable at high mobility ratios (unfavorable) and for low values of the permeability variation coefficient, V_{DP} (less heterogeneous reservoirs).
4. The injectivity ratio is governed by the effective mobility ratio at early times and by the conventional mobility ratio at later times. The injectivity ratio for BL displacement is always less than that for PL displacement. with the difference increasing at high (unfavorable) mobility ratios. The injectivity ratio increses as the reservor heterogeneity (V_{DP}) and viscosity ratio increase. The ultimate value of the injectivity ratio is equal to the PL mobility ratio.
5. The fractional flow and pseudo relative perrmeability formulas derivrd for the model cant be used for simulation of the entire system. These functions correspond only to the conditions at the outlet face at different times.

Nomenclature

A = area, L^2, ft^2 [m^2]
C_t = total formation capacity, L^3, md. Ft[
f_W = water cut, dimensionless
f_w* = water cut at breakthrough, dimensionless
h_t = total formation thickness, L, ft [m]
Δh = formation thickness of a layer, L, ft [m]
I_R = injectivity ratio, dimensionless
k = absolute horizontal permeability, L^2, md [μm^2]
k_{ro}^{o} = oil relative permeability at S_{wi} , dimensionless
$\tilde{k}_{ro}$ = pseudo relative permeability for oil, dimensionless
k_{rw}^{o} = water relative permeability at S_{or} , dimensionless
$\tilde{k}_{rw}$ = pseudo rel. permeability for water, dimensionless
L = length, L, ft [m]
n = number of layers
ΔP = pressure drop, M/ Lt, psi[kPa]
Q = flow rate, L^3/ t , bbl/d [m^3/s]
R = vertical coverage, dimensionless
S_D = dimensionless water saturation
S_{or} = residual oil saturation, fraction
S_W = water saturation, fraction
S_{wi} = initial water saturation, fraction
ΔS = displaceable oil saturation, fraction
t = time, t, d [s]
V_{DP} = Dykstra–Parsons variation coefficient,
x = distance from inlet face , L, ft [m]
X_f = dimensionless distance of the displacement front
Υ = mobility ratio , dimensionless
η = function defined by Eq.(A-30)
λ = phase mobility, Lt/M, cp^{-1} [1/Pa.s]
μ = viscosity, m/Lt, cp.[Pa.s]
τ = dimensionless time
φ = porosity, fraction

Subscripts

i = initial , irreducible
D = dimensionless
m = mean
o = oil
r = relative
t = total
w = water

Superscripts

* = breakthrough
‘ = derivative
- = average
~ = pseudo

Acknowledgement

The author wishes to acknowledge the support provided by the Petroleum Engineering Department of King Saud University during this study.

References

1. Buckley, S.E. and Leverett, M.C.: "Mechanism of Fluid Displacement in Sands," *Trans.*, AIME (1942) **146**, 107.
2. Welge, H.J.: "A Simplified Method for Computing Oil Recovery by Gas or Water Drive," *Trans.*, AIME (1952) **195**, 91–98.
3. Stiles, W.E.: "Use of Permeability Distribution in Water-flood Calculations," *Trans.*, AIME (1949) **186**, 9-13.
4. Dykstra, H. and parsons, R.L.: "The Prediction of Oil recovery by Waterflooding," *Secondary Recovery of Oil in the United States*, 2nd ed., API (1950) 160–174.
5. Hiatt, N.W.: "Injected–fluid Coverage of Multi–well Reservoirs with Permeability Stratification," *Drill and Prod. Prac.*, API (1958) **165**, 165–194.
6. Warren, J.E. and Cosgrove, J.J.: "Prediction of Waterflood Behavior in a Stratified System," *Soc. Pet. Eng. J.* (June 1964) 149–157.
7. Hearn, C.L.: "Simulation of Stratified Waterflooding by Pseudo Relative Permeability Curves," *J. Pet. Tech.* (July 1971), 805–813.
8. Reznik, A.A., Enick, R.M. and Panvelker, S.B.: "An Analytical Extension of the Dykstra–Parsons Vertical Stratification Discrete Solution to a Continuous, Real–Time Basis," *Soc. Pet. Eng. J.* (1984) **24**, 643–656.
9. El–Khatib, N.A.: "The Effect of Crossflow on Waterflooding of Stratified Reservsoirs," *Soc. Pet. Eng. J.* (April, 1985), 291–302.
10. El–Khatib, N.A.: "Waterflooding Performance of Communicating Stratified Reservoirs with Log-Normal Permeability Distribution," *SPEREE* (Dec. 1999) **2**,542-49.
11. Willhite, P.G.: *Waterflooding*, SPE Textbook Series, Vol 3, Richardson,TX. (1986) 139-45.
12. Snyder, R.W. and Ramey, H.J. Jr.: "Applications of Buckley-Leverett Displacement Theory to Noncommunicating Layered Systems," *J. Pet. Tech.* (Nov. 1967), 1500-06.
13. Pande, K.K., Ramey, H. J. Jr., Brigham, W.E. and Orr, F.M. Jr.: "Frontal Advance Theory for Flow in Heterogeneous Porous Media, paper SPE 16344 presented at SPE California Regional Meeting, Ventura, California, April 8–10, 1987.

Appendix
Derivation of the Mathematical Model
Performance before Water Breakthrough

Figure A-1 shows the saturation distribution in before water breakthrough a typical layer.

The the frontal advance formula for any layer i is

$$\frac{dx_{fi}}{dt} = \frac{q_{ti}}{A_i \varphi} \frac{df_w^*}{dS_w} \qquad \text{(A-1)}$$

For uniform initial saturation distribution at the irreducible water saturation Sw_I , Eq.(A-1) is integrated giving

$$X_i = t_{di} \frac{df_w}{dS_w} \qquad \text{(A-2)}$$

where X is dimensionless distance (x/L) moved by a constant saturation at dimensionless time t_{di} which is the water injected in the i^{th} layer expressed in terms of pore volume of that layer.

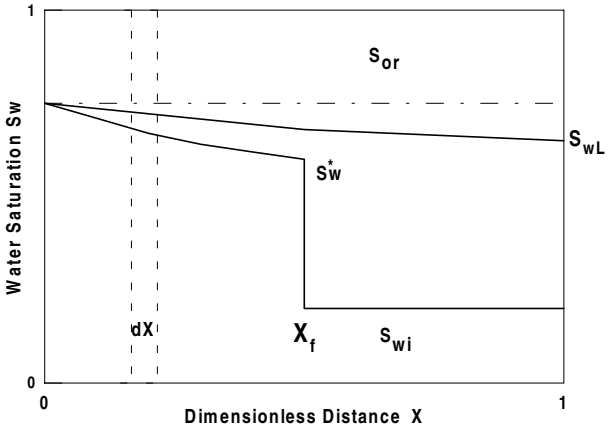

Fig. A-1 - Saturation Distribution before and after Breakthrough

$$t_{Di} = \frac{\int_0^t q_{ti} dz}{A_i \varphi L} \qquad \text{(A-3)}$$

2- The dimensionless time of breakthrough, t^*_D , which is the pore volume injected in a layer at time of breakthrough.

The location of the displacement front in the i^{th} layer, X_{fi} is given by

$$X_{fi} = t_{di} \left(\frac{df_w^*}{dS_w}\right) = \frac{t_{di}}{t_d^*} \qquad \text{(A-4)}$$

where t^*_D is the dimensionless time of breakthrough. This is the same for all layers and is the recoprical of the slope of the tanfent to the fractional flow curve from the point of initial conditions ($S_{wi,}$ 0).

$$t_D^* = \frac{1}{\frac{df_w^*}{ds_w}} \qquad \text{(A-5)}$$

The total pressure drop which is the same across all layers is obtained using Darcy law

$$\Delta P_t = \frac{q_{ti} L}{k_i A_i} \int_0^1 \frac{dX}{\lambda_t} \qquad \text{(A-6)}$$

Noting that λ_t in the uninvaded zone is constant at λ_o^0 and from the frontal advance theory, X in the invaded zone is given by Eq.(A-4), Eq.(A-6) can be written as

$$\Delta P_t = \frac{q_{ti} L}{k_i A_i}\{t_{Di}\int_0^{f_w'^*}\frac{df_w'}{\lambda_t} + \frac{1-X_{fi}}{\lambda_o^0}\} \qquad \text{(A-7)}$$

Using the following definition of average total mobility

$$\frac{1}{\bar{\lambda}_t} = \frac{\int_o^{f_w'^*}\frac{df_w'}{\lambda_t}}{f_w'^*} = t_D^* I^* \qquad \text{(A-8)}$$

where

$$I(x) = \int_o^x \frac{df_w'}{\lambda_t} \qquad \text{(A-9)}$$

and

$$I^* = I(1/t_D^*) = \int_o^{f_w^*}\frac{df_w'}{\lambda_t} \qquad \text{(A-10)}$$

equation (A-7) becomes

$$\Delta P_t = \frac{q_{ti} L}{k_i A_i}\{\frac{X_f}{\bar{\lambda}_t} + \frac{1-X_{fi}}{\lambda_o^0}\} \qquad \text{(A-11)}$$

Defining an effective mobility ratio as

$$\bar{\gamma} = \frac{\bar{\lambda}_t}{\lambda_o^\circ} \qquad \text{(A-12)}$$

equation (A-11) may be arranged for the total flow rate as

$$q_{ti} = \frac{k_i A_i \lambda_o^0 \Delta P_t}{L(1-(\frac{\bar{\gamma}-1}{\bar{\gamma}})X_{fi})} \qquad \text{(A-13)}$$

Equation (A-13) is similar to the equation used in deriving the location of the displacement front in the Dykstra-Parsons model with the modified mobilty ratio $\bar{\gamma}$ replacing the conventional mobility ratio γ defined as

$$\gamma = \frac{\lambda_w^0}{\lambda_o^0} = \frac{k_{rw}^0}{k_{ro}^0}\frac{\mu_o}{\mu_w} \qquad \text{(A-14)}$$

So the following equations can be used (see ref. ,9)
Before water breakthrough in the first(most permeable) layer, the location of the displacement front in any layer j ,X_{fj} in terms of X_{f1} is given by

$$X_{fi} = (\frac{\bar{\gamma}}{\bar{\gamma}-1})[1-\sqrt{1-2(\frac{\bar{\gamma}-1}{\bar{\gamma}})\frac{k_i}{k_1}(X_1-(\frac{\bar{\gamma}-1}{2\bar{\gamma}})X_1^2)}] \qquad \text{(A-15)}$$

Equation (A-15) may br used to obtain the front location in layer i in terms of that in any layer j by replacing k_1 by k_j and X_1 by X_j.

The dimensionless time of the different layers is given by

$$t_{Di} = X_{fi} t_D^* \qquad \text{(A-16)}$$

The fractional oil recovery R and total dimensionless time τ are given by

$$R = \tau \qquad \text{(A-17)}$$

$$\tau = \frac{\sum_{i=1}^n t_{Di}\Delta h_i}{h_t} \qquad \text{(A-18)}$$

where the total dimensionless time τ is based on the total pore volume of the system

$$\tau = \frac{\int_0^t \sum_{i=1}^n q_{ti} dz}{A_t \varphi L} \qquad \text{(A-19)}$$

The expression for the injectivity ratio I_R is

$$I_R = \frac{1}{c_t}\sum_{i=1}^n \frac{k_i \Delta h_i}{1-(\frac{\bar{\gamma}-1}{\bar{\gamma}})X_{fi}} \qquad \text{(A-20)}$$

where c_t is the total formation capacity

$$c_t = \sum_{i=1}^n k_i \Delta h_i \qquad \text{(A-21)}$$

During this period

$$f_w = 0 \qquad \text{(A-22)}$$

To convert to real time for the case of constant totat pressure drop , Substituting for q_t from Eq.(A-13) into the frontal advance formula, Eq.(A-1) and and using X=x/l , we get

$$\frac{dX_{fi}}{dt} = \frac{k_t \lambda_o^0 \Delta P_t}{L^2 \varphi (1-(\frac{\bar{\gamma}-1}{\bar{\gamma}})X_{fi})}\frac{df_w^*}{dS_w} \qquad \text{(A-23)}$$

Integrating Eq.(A-23) and rearranging we obtain

$$t = \frac{L^2 \varphi\, t_D^*}{k_i \lambda_o^0 \Delta P_t}[X_i - (\frac{\bar{\gamma}-1}{2\bar{\gamma}})X_i^2] \qquad \text{(A-24)}$$

The time of breakthrough in layer i is obtained by setting X_i=1

$$t_i^* = (\frac{\bar{\gamma}+1}{2\bar{\gamma}})\frac{L^2 \varphi\, t_D^*}{k_i \lambda_o^0 \Delta P_t} \qquad \text{(A-25)}$$

Performance after Water Breakthrough. After water breakthrough in a layer i, the total pressure drop across the

layer is obtained by substituting Eq.(A-2) into Eq.(A-6) and noting that at X=1, $f_w' = 1/t_{Di}$

$$\Delta P_t = \frac{q_{ti}L}{k_i A_i} t_{Di} \int_0^{f_w'=1/t_{Di}} \frac{df_w'}{\lambda_t} \quad \text{(A-26)}$$

Using the definition for the integral I as given by Eq.(A-9) , equation(A-26) may be written as

$$q_{ti} = \frac{k_i A_i \lambda_o^0 \Delta P_t}{L\left(\lambda_o^0 t_{Di} I(1/t_{Di})\right)} \quad \text{(A-27)}$$

Since

$$dt_{Di} = \frac{q_{ti}dt}{A_i \varphi L} \quad \text{(A-28)}$$

then for two layers i and j , both after breakyhrough

$$\frac{dt_{Di}}{dt_{Dj}} = \frac{k_i}{k_j} \frac{t_{Dj} I(1/t_{Dj})}{t_{Di} I(1/t_{Di})} \quad \text{(A-29)}$$

Integrating this equation for a given interval of real time and defining a function η as

$$\eta(z) = \int_{t_D^*}^{z} t_D I(1/t_D) dt_d \quad \text{(A-30)}$$

the integration may be written as

$$\Delta\eta_i = \frac{k_i}{k_j} \Delta\eta_j \quad \text{(A-31)}$$

At the time of breakthrough in layer j, the location of the displacement front for lyer i (j<i≤n) is obtained from Eq.(A-15) by replacing 1 by j and setting X_j=1

$$X_{fi} = \left(\frac{\bar{\gamma}}{\bar{\gamma}-1}\right)\left[1 - \sqrt{1 - \left(\frac{\bar{\gamma}-1}{\bar{\gamma}}\right)\frac{k_i}{k_j}}\right] \quad \text{(A-32)}$$

For the two layers i after and j before breakthrough , from Eqs. (A-13) and (A-27) and (A-28) we get

$$\frac{dt_{Di}}{dt_{Dj}} = \frac{k_i}{k_j} \frac{1 - \left(\frac{\bar{\gamma}^2 - 1}{\bar{\gamma}^2}\right)\frac{t_{Dj}}{t_D^*}}{t_{Di} I(1/t_{Di})} \quad \text{(A-33)}$$

Setting i=j-1 and integrating from time of breakthrough in layer j-1($t_D = X_{fi}\, t_D^*$ where X_{fi} is given be Eq(A-32)) and time of breakthrough in layer j ($t_D = t_D^*$), the following equation is obtained

$$\Delta\eta_{j-1} = \eta_{j-1} = \frac{t_D^*}{\lambda_o^0}\left(\frac{\bar{\gamma}+1}{2\bar{\gamma}}\right)\left[\frac{k_{j-i}}{k_j} - 1\right] \quad \text{(A-34)}$$

Applying Eq.(A-31) to layers i≤j-1 we get

$$\Delta\eta_i = \frac{k_i}{k_{j-1}} \Delta\eta_{j-1} \quad \text{(A-35)}$$

and

$$\eta_i = \eta_{i\,old} + \Delta\eta_i \quad \text{(A-36)}$$

To convert to real time, substituting for q_t from Eq.(A-27) into Eq.(A-28)

$$dt_{Di} = \frac{k_i \Delta P_t}{\varphi L^2 \left(t_{Di} I(1/t_{Di})\right)} dt \quad \text{(A-37)}$$

Integtating from time of breakthrough t_i^* to any time t

$$t = t_i^* + \frac{L^2 \varphi}{k_i \Delta P_t} \eta_i \quad \text{(A-38)}$$

where t_i^* is given by Eq.(A-25)

SI Metric Conversion Factors

bbl	x	1.589 873	E – 01 = m^3
cp	x	1.0*	E – 03 = Pa.s
ft	x	3.048*	E – 01 = m
ft^2	x	9.290 304*	E – 02 = m^2

*Conversion factor is exact.